PROCEEDINGS, 50th Workshop on Geothermal Reservoir Engineering
Stanford University, Stanford, California, February 10-12, 2025
SGP-TR-229

Long-term Monitoring and Performance Evaluation of ATES-GSHP System in Esker Formation: Case Study in Stockholm

Mohammad Abuasbeh, Björn Palm

Royal Institute of Technology (KTH), Department of Energy Technology, 10044 Stockholm, Sweden

abuasbeh@kth.se

Keywords: Aquifer Thermal Energy Storage, Ground Source Heat Pump, Long Term Performance Analysis, Shallow Geothermal Energy

ABSTRACT

This study aims to conduct a long-term (since 2016) performance evaluation of the doublet-type Aquifer Thermal Energy Storage (ATES) system located in Esker geological formation in Stockholm, Sweden. Furthermore, the ATES is connected to a ground source heat pump (GSHP). The average annual heating and cooling used from the ATES are 158 MWh and 243 MWh respectively during the first 3 annual storage cycles of operation. The licensed amount of water extraction and injection is 50 liters per second with an undisturbed groundwater temperature of 9.5 ◦C. Over the first three storage cycles, the average injection and extraction temperatures for the warm side are 13.3 ◦C and 12.1 ◦C, and for the cold side 7.6 ◦C and 10.5 ◦C. The average temperature differences across the main heat exchanger from the ATES side are 4.5 K during winter and 2.8 K during summer which is 4-5 degrees lower than the optimum value. The data analysis indicated annual energy and hydraulic imbalances, resulting in undesirable thermal breakthroughs between the warm and cold sides of the aquifer. This was mainly due to suboptimal operation of the building energy system which led to insufficient heat recovery from the warm side, and subsequently insufficient cold injection in the cold wells, despite the building heating demand and the available suitable temperatures in the ATES. The cause of the suboptimal operation is the oversizing of the heat pumps which were designed to be coupled to larger thermal loads as compared to the ones in the final system implementation. As a result, the heat pumps could not be operated during small-medium loads. The seasonal performance factor (SPF) of the GSHP-ATES ranges between 24-53 for free heating and cooling mode and between 4.5-6.5 when coupled with the heat pump. Additionally, the paper proposes an additional thermal KPI named heat exchanger efficiency balance (β_{HEX}) that connects and evaluates the optimum operational point of temperature differences from both the building and ATES perspective. In addition to ATES energy and hydraulic KPIs, β_{HEX} can contribute to providing a more complete picture of the ATES-building interaction performance as well as highlight if the losses in energy recovery from ATES are due to the subsurface processes or building energy system operation which has been proven to be critical for the optimum ATES performance.

1. INTRODUCTION

With increasing effort worldwide to reduce the carbon footprint and impact on environment, most country has been investing in more sustainable solution in the energy sector. In most industrial countries, energy consumed by building sector reaches up to 40% of their total final energy consumption (Pérez-Lombard et al., 2008). The total energy consumption by the residential and commercial sector in 2017 amount to nearly 40% of the total energy used in the USA (USEIA, 2020), of which nearly half is consumed for heat and cooling buildings (Pérez-Lombard et al., 2008). The residential and services (including commercial buildings) sector in Sweden is responsible for 147 TWh or 35% of the country's total energy consumption in 2018. Half of which has been used for space heating and domestic hot water, cooling (Energimyndighetens, 2020). Therefore, significant efforts have been invested in increasing the efficiency of HVAC systems, energy storage technologies as well as reducing the building energy demand. Low temperature thermal energy storage applications, both for heating and cooling purposes, have attracted more and more attention in the recent years. Aquifer thermal energy storage (ATES) has drawn particular interest when it comes to long-term (usually seasonal) and short-term thermal energy storage due to its economic feasibility and short payback time compared to other thermal storage alternatives. This is mainly because ATES enables the use of groundwater as storage medium. Water is favorable thermal storage medium since it has relatively high specific heat and low thermal conductivity. In spite of these efforts invested to improve HVAC systems' efficiency, it is more often that the actual building energy consumption exceeds the designed values in what referred to in literature as "performance gap" (de Wilde, 2014; Imam et al., 2017; Liang et al., 2019; Menezes et al., 2012). This can lead to the so called green or low energy building actual performance not being as low energy as anticipated. Large study conducted in New York evaluating 953 building of which included 21 LEED certified buildings revealed that there were no energy saving difference between the LEED certified buildings and the non-LEED certified ones (Scofield, 2013). Another study conducted in Sweden that included 21 buildings built between 2002-2013 concluded that a performance gap that exceeded 20% relative to the design values (Kurkinen, 2014). Furthermore, the study reported performance gap values of up to 250% mentioned in literature for an addition 20 buildings built between 1988 -2014 in Sweden and the Nordic countries. These studies usually use the energy use intensity (EUI) as the main indicator for the building performance mainly for its simplicity since it does not require other that the floor area of the building and its total energy bill. Such a measure would give a general indication about the building performance, but lacks the information about the causes behind any inefficiencies in this building. Such information cannot be obtained without more comprehensive instrumentation and evaluation of the building HVAC system components. Very few studies exist in literature about regarding long term monitoring and evaluation of HVAC system on more detailed component level to compare with (Spitler & Gehlin,

2019). Though with the cost of sensors becoming cheaper, the possibility to instrument, collected more detailed data and evaluate the energy system in buildings becomes more accessible. (Spitler & Gehlin, 2019) conducted the review of 55 ground source heat pumps (GSHP) systems that reported seasonal performance factors (SPF), based on SEPEMO boundaries, for a period of one year or more. SEPEMO is a commonly used standard, which consists of four levels of SPFs for each heating and cooling. Level 1 covers the heat pump unit, level2 add in the source side, level 3 includes any auxiliary heating and level 4 include the circulation pumps and fans on the load side (see level 1 and level 2 in Fig 3). The review concluded that very few cases presented SPF values for level 4 and only 3 present uncertainty analysis. Additionally, the reported values were mostly yearly values of SPF without presenting monthly values. (Gleeson & Lowe, 2013) conducted a study that included GSHP systems in residential buildings and reported significant differences in SPF values that could not be explained by only the different choice of equipment or conditions of the climate. This indicates that the operation protocol of the system of during heating and cooling have a significant influence on the final system performance. In (Spitler & Gehlin, 2019) study they provided a case study, based on SEPEMO boundaries, of a long-term detailed monitoring and evaluation of the borehole GSHP system in a university building in Stockholm. They included monthly SPFs as well as a detailed methodology for uncertainty analysis. Considering SEPEMO, the heating SPF for boundaries 2 and 3 was reported to be 3.7± 0.2 and 2.7± 0.13. For cooling SPF2, the value achieved was 27± 0.13. In this case study, the building GSHP system has been designed, fully instrumented and monitored by experienced owners and staff. This resulted in consistent operation SPF for heating with the design values where the cooling SPF was four times the design value. This clearly highlights the importance of proper instrumentation and long-term monitoring of energy systems in buildings and its effect on improved performance.

When it comes to ATES-GSHP systems, detailed and long-term monitoring data is scarce in the literature. (Schmidt & Müller-Steinhagen, 2004) reported the Seasonal heating COP of the heat pump only for 3 years averaging 4.3. Their system consisted of a 7000 m2 residential building in Germany. The heating and cooling system consisted of solar collectors, a gas-fired boiler, and ATES coupled with heat pumps. (Vanhoudt et al., 2011) conducted a three-year monitoring study on an ATES-GSHP system that provides heating and cooling for a hospital in Belgium. They reported SPF values for the heat pump of 5.6 and 5.0 for heating and cooling respectively. SPFs of the system reported averaging of 5.9 and 26.1 for heating and cooling. The boundaries at which these values are calculated are not clear and whether any circulation pumps were included or not is not clear.

Furthermore, the boundaries for system components chosen for evaluation can vary between different studies making it more difficult for comparison. (Spitler & Gehlin, 2019) conducted a comprehensive review of several standards of system boundaries to calculate the SPFs for different boundary levels within the building system commonly using GSHP. While it is commonly used, SEPEMO standard is most suitable for residential buildings where it has relatively low complexity and similar energy system components. This facilitates comparing different installations. But when applying it to commercial or large scale system with higher complexity in term of system component design and operation protocol, SEPEMO boundaries might not be always applicable.

This study aims to present the monitoring data and long-term performance evaluation of an ATES-GSHP system in esker formation located in Solna, Stockholm. A preliminary evaluation of the ATES and comprehensive details about the monitoring systems of both the subsurface and the building energy system have been previously published by (Abuasbeh & Acuna, 2018).

2. DESCRIPTION OF THE INSTALLATION

The study area is located in the northern part of Stockholm, at the north-western side of Lake Brunnsviken, by the E4 highway (see Figure.1). The ATES system is positioned on the Stockholm esker in a property that consist of two office buildings with total heated area of approximately 18,000 m2. The ATES system is connected to two Carrier heat pumps with total cooling capacity of around 1.5 MW. The ATES consists of four warm wells in the northern side of the property (BV01-04 in fig 1), one of which is not currently used, and two cold wells in the south of the property (BK01-02 in fig 1). The ATES has been in operation since autumn 2016. The allowed pumping flow rate for both extraction and injection of groundwater is up to 50 l/s. The estimated saturated thickness of the aquifer ranges between 20m near the cold side to 7.5m in the warm side. The estimated distance between the center of the cold wells and the warm wells groups' centers is 90 m.

Figure 1: Image showing the esker passing through the property (left) and a zoomed in image showing the two buildings and the ATES wells (right).

The main geological feature is the Stockholm esker stretching nearly in the north- northwest direction. The landscape is under the level of the highest marine shoreline giving a more complex soil stratigraphy with deposits of clay but also remains of relic saltwater (Boman & Hanson, 2004). The top of the ridge of the esker has partly been subject to excavation due to a former use as gravel pit. The core of the esker is passing through the southern side of the property. Depth from surface to bedrock within the property ranges from 12 to 20 m and aquifer thickness ranges from 8 to 15 m from north to south. The hydraulic conductivity of the esker was estimated from pumping tests to be in the range of 2.5-2.9*10^{-3} *m/s*. During a pumping test carried out over 35 days with a stable flow of 27 *l/s*, transmissivity estimates ranges were 4.0-5.8 *10^{-3} m^2/s. Drillings had shown that the main geological material in the esker comprises sand and gravel. However, at the northern part, it was presented that the aquifer has fillings of finer grained material as silt (WSP, 2014).

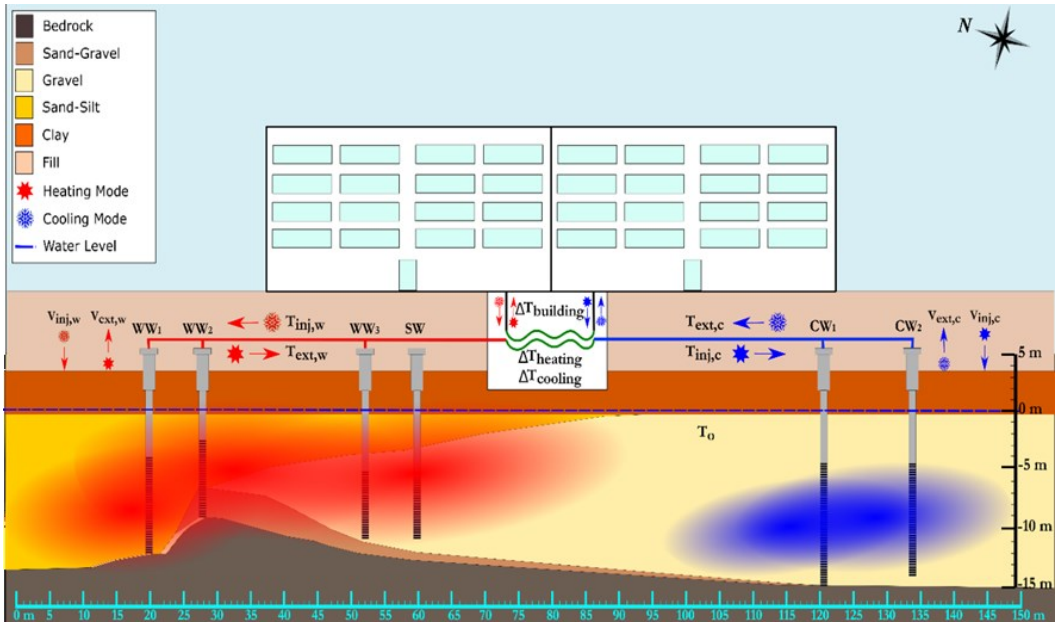

Figure 2: Cross-section along the esker showing positions of the wells as well as the operation modes of the ATES.

In Figure 2, the system and the measured variables used in this paper are illustrated. The acronyms ***WW*** refer to warm well, ***CW*** refer to cold well and ***SW*** refer to spare well. The temperature acronyms $T_{inj,w}$, $T_{ext,w}$, $V_{inj,w}$ and $V_{ext,w}$ refer to the injection and extraction temperatures and volume flowrates in the warm wells group where $T_{inj,c}$, $T_{ext,c}$, $V_{inj,c}$ and $V_{ext,c}$ refer to the injection and extraction temperatures and volume flowrates in the cold wells group. Furthermore, $\Delta T_{heating}$, $\Delta T_{cooling}$ and T_o refer to the temperature difference across the inlet and outlet of the heat exchanger from the ATES side during heating and cooling mode and the undisturbed temperature of the aquifer respectively. $\Delta T_{building}$ refer to the temperature difference across the inlet and outlet of the heat exchanger from the building side.

2.1 Heating and cooling system operation modes

***Heating*:** during which the heat pumps are used to supply heating towards the building heating distribution network and domestic hot water while using district heating as a backup. On the heat pump evaporator side, the heat source is being divided between the ATES and the building cooling distribution network. This means that while heating, the heat pump is simultaneously cooling the building as well.

***Free cooling*:** during which the ATES provides direct cooling (without the use of the heat pumps) towards the building cooling distribution network and domestic hot water demand is supplied using district heating.

***Machine cooling*:** during which the heat pumps are used to supply cooling towards the building cooling distribution network and domestic hot water demand usually supplied by the heat pumps condenser while using district heating as a backup. The excess heat from the condenser is rejected to air chillers on the roof. This means that during machine cooling, there will be some form of heating as well.

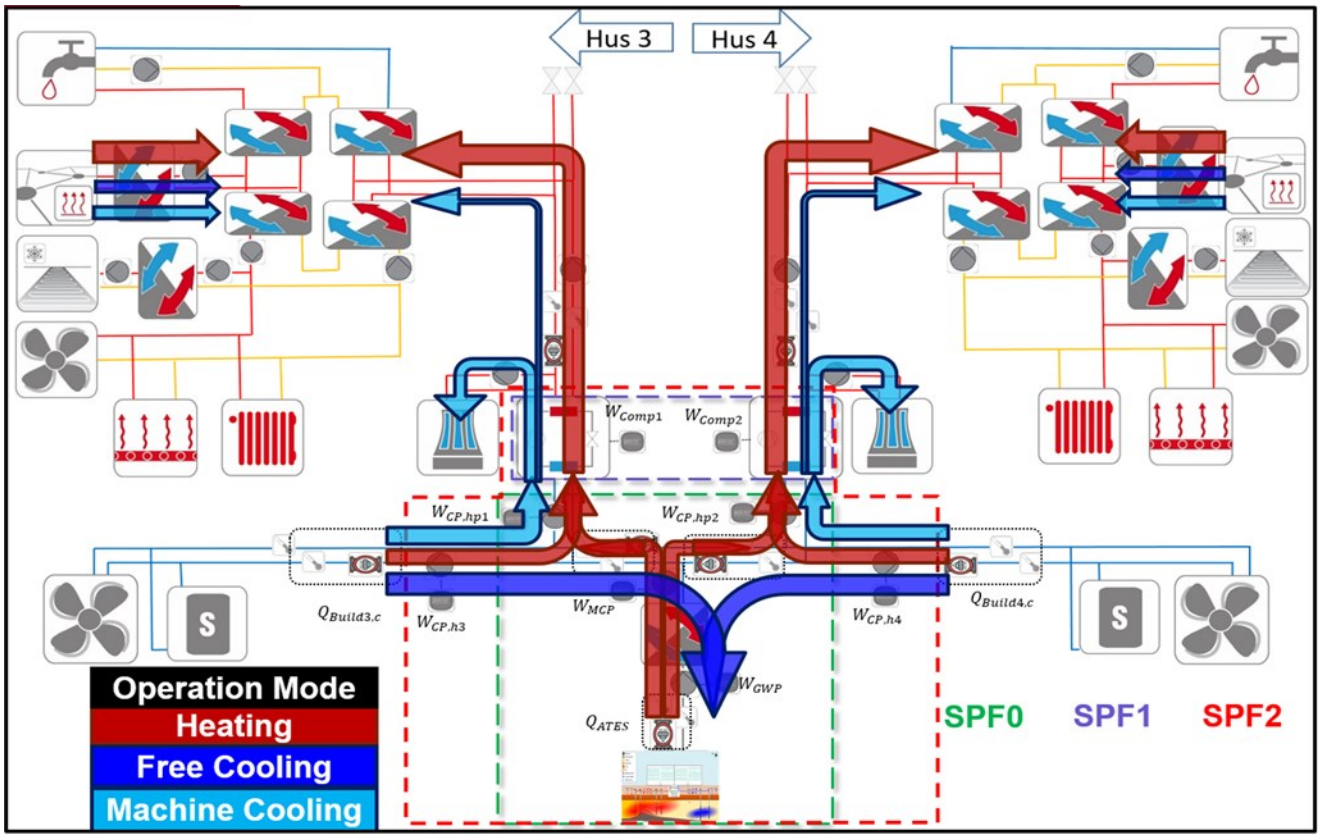

Figure 3: Schematic of the heating and cooling system in Solna with the boundary levels for SPF0-SPF2 showing the energy flow in each the main operation conditions, heating (red arrow), free cooling (dark blue arrow) and machine cooling (light blue arrow). The ATES location in the system is represented by the small schematic at the middle bottom part of the figure.

3. SYSTEM KEY PERFORMANCE INDICATORS DEFINITION

To evaluate the heating and cooling system, we will use the seasonal performance factor (SPF) or monthly performance factor (MPF) as the main key performance indicator. SPF is defined by the following equation.

$$SPF = \frac{\sum Q_{thermal}}{\sum W_{electrical}} \quad (1)$$

Where $Q_{thermal}$ is the thermal energy utilized for heating or cooling during the season (usually a year), and $W_{electrical}$ is the electrical energy consumed in order to deliver the heating or cooling demand during that period of time.

Each of boundary levels describe a certain group of components of the system. SPF_0, SPF_1, and SPF_2, are the ATES, heat pump circuits, and the combined ATES-GSHP loop respectively as shown in figure 3. The subscripts (C) and (H) indicate cooling and heating operation respectively. The *SPFs* are defined by the following equations

$$SPF_{C0} = \frac{Q_{ATES,c}}{W_{GWP,fcm} + W_{MCP,fcm} + W_{CP,hp}} \quad , \quad SPF_{H0} = \frac{Q_{ATES,h}}{W_{GWP,hm} + W_{MCP,hm} + W_{CP,hp}} \quad (2)\ ,\ (3)$$

$$SPF_{C1} = \frac{Q_{Evap}}{W_{Comp}} \quad , \quad SPF_{C1} = \frac{Q_{Evap}}{W_{Comp}} \quad (4)\ ,\ (5)$$

$$SPF_{C2} = \frac{Q_{Build,c}}{W_{GWP,fcm} + W_{MCP,fcm} + W_{CP,hp,mcm} + W_{Comp,c}} \quad , \quad SPF_{H2} = \frac{Q_{Cond}}{W_{GWP,hm} + W_{MCP,hm} + W_{CP,hp,hm} + W_{Comp,hm}} \quad (6)\ ,\ (7)$$

Where W_{GWP}, W_{MCP}, W_{CP}, W_{Comp} indicate the electrical energy consumption the ground water pumps from the Aquifer, the main circulation pump connecting the ATES to the heating system, a circulation pump, and the heat pumps compressor respectively. The subscripts (*fcm*), (*hm*), (*mcm*), and (*hp*) indicate free cooling mode, heating mode, machine cooling mode, and heat pump related component. Q_{ATES}, Q_{Evap}, Q_{Cond}, Q_{Build} indicate the thermal energy exchanged with the ATES, heat pump evaporator, heat pump condenser, and the building cooling network respectively as shown in figure 3.

3.1 ATES Key Performance Indicators Definition

The heat exchanger efficiency (η_{HEX}) proposed by (Abuasbeh et al., 2021) describes how much of the maximum possible temperature difference across the heat exchanger has been utilized. This efficiency can be describe from both point of view of the building ($\eta_{HEX_{build}}$) or the ATES ($\eta_{HEX_{ATES}}$). They can be formulated as the ratio between the temperature difference between the inlet and the outlet of the heat exchanger, from either the building or the ATES side, and the temperature difference between the inlets of the heat exchanger from each side as shown in the equations (8) and (9). Furthermore, the heat exchanger efficiency balance for both sides can be introduced and formulated as shown in equation (10).

$$\eta_{HEX_{build}} = \frac{\left|T_{Build_{HEX_{Out}}} - T_{Build_{HEX_{In}}}\right|}{\left|T_{Build_{HEX_{In}}} - T_{ATES_{HEX_{In}}}\right|} \quad , \quad \eta_{HEX_{ATES}} = \frac{\left|T_{ATES_{HEX_{Out}}} - T_{ATES_{HEX_{In}}}\right|}{\left|T_{Build_{HEX_{In}}} - T_{ATES_{HEX_{In}}}\right|} \quad (8)\ ,\ (9)$$

$$\beta_{HEX} = \frac{\eta_{HEX_{build}} - \eta_{HEX_{ATES}}}{\eta_{HEX_{build}} + \eta_{HEX_{ATES}}} \quad (20)$$

Where $T_{build_{HEX_{In}}}$, $T_{build_{HEX_{Out}}}$, $T_{ATES_{HEX_{In}}}$ and $T_{ATES_{HEX_{Out}}}$ are the inlet and the outlet temperatures from the main heat exchanger from the building and ATES side respectively. Ideally, the temperature difference across the heat exchanger from the building side and the ATES is desired to be as high as possible. High-temperature difference from the building side ($\Delta T_{building}$) leads to the warmest (or coldest during summer) forward temperature during winter towards the building heating system. Similarly, a high-temperature difference from the ATES side ($\Delta T_{heating}$ or $\Delta T_{cooling}$) leads to the coldest (or warmest during summer) injection temperature during winter in the ATES which improves the storage for the following season. The heat exchanger efficiency balance (β_{HEX}) would have a value of range between 1 and -1. Where a negative value would mean that the operation over the main heat exchanger is more optimized in favor of the building system and a positive value would mean that the operation is in favor of the ATES. These efficiencies provide insight into how optimum the system operation has been from the point of view of the ATES and building heating and cooling.

4. RESULTS

This study presents the monitoring data from ATES-GSHP system, performance analysis and systems boundaries evaluation of the heating and cooling systems during the selected period March 2019 – April 2020. The installation has been in operation since 2016, but the detailed data (mainly for the heat pumps) to evaluate the different SPFs was not available. The only exception is SPF_0, for which sufficient measurement has been obtained since October 2016. Therefore, SPF_0 results will be presented for the period between October 2016 – April 2020.

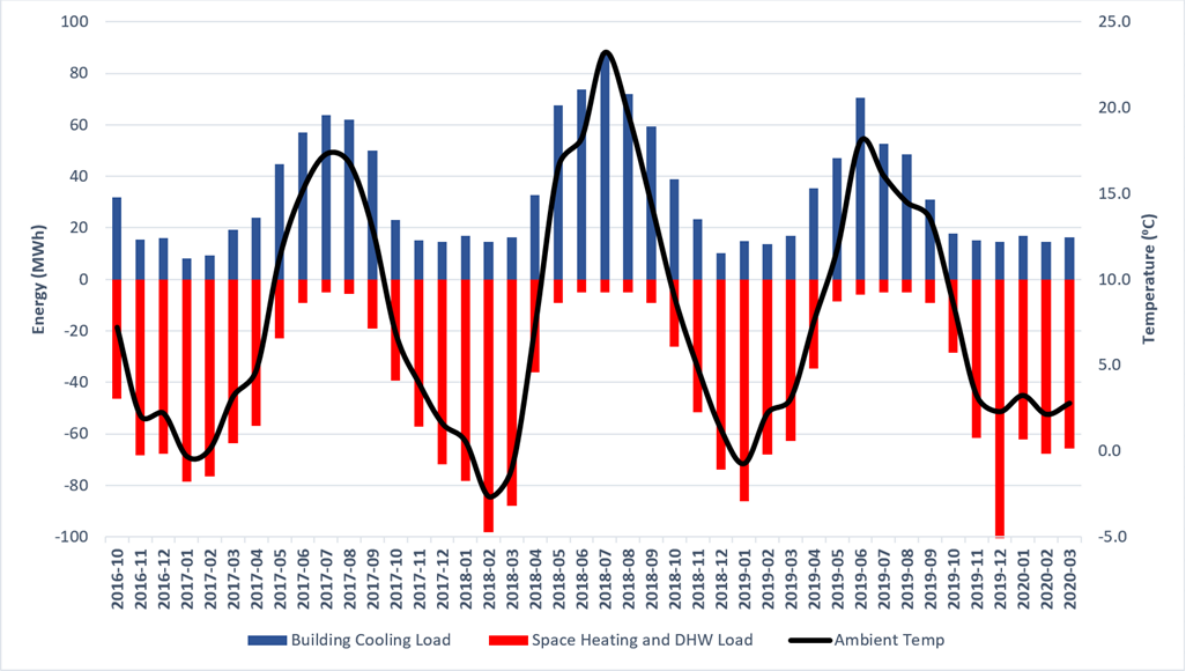

Figure 4: Monthly Building Cooling, Space Heating & Domestic Hot Water Load in MWh, and the average ambient temperature.

For the period April 2019-April 2020, the total heating (including space heating and domestic hot water) and cooling demand was 456 MWh and 380 MWh. The aggregated monthly values are shown in **Error! Reference source not found.**. The total heated and cooled area in both buildings is around 18000 m^2. This give energy usage intensity (EUI) values of 25 (kWh/m^2) and 21 (kWh/m^2). When designed, the building heating and cooling system was meant to have heating and cooling energy intensity of 40(kWh/m^2), and 50 (kWh/m^2) when including electricity consumption, compare to the measured 46 (kWh/m^2). The system seem to have a very decent value of EUI, we can still notice a performance gap which might lead to the building being just shy of the Platinum LEED certification requirement (51 kWh/m^2).

Table 1: Overall load characteristics

Start of evaluation period	Oct 2016	Oct 2017	Oct 2018	Oct 2019
End of evaluation period	Sep 2017	Sep 2018	Sep 2019	March 2020
Building space heating + DHW load met by system [MWh_{th}]	520	502	437	387
Building cooling load met by system [MWh_{th}]	401	494	404	95
Thermal energy extracted from the ground [MWh_{th}]	189	169	115	83
Thermal energy injected to the ground [MWh_{th}]	235	236	272	9
Thermal balance ratio (extracted/rejected)	0.80	0.72	0.42	9.22
Heating load (incl. DHW) met by ATES (%)	36	34	26	21
Cooling load met by ATES (%)	59	48	67	9

4.1 Heat Pump Performance

The heat pump data analyzed in this study is for the period April 2019- March 2020. The heat pump operation evaluation is done in system boundary SPF_1.

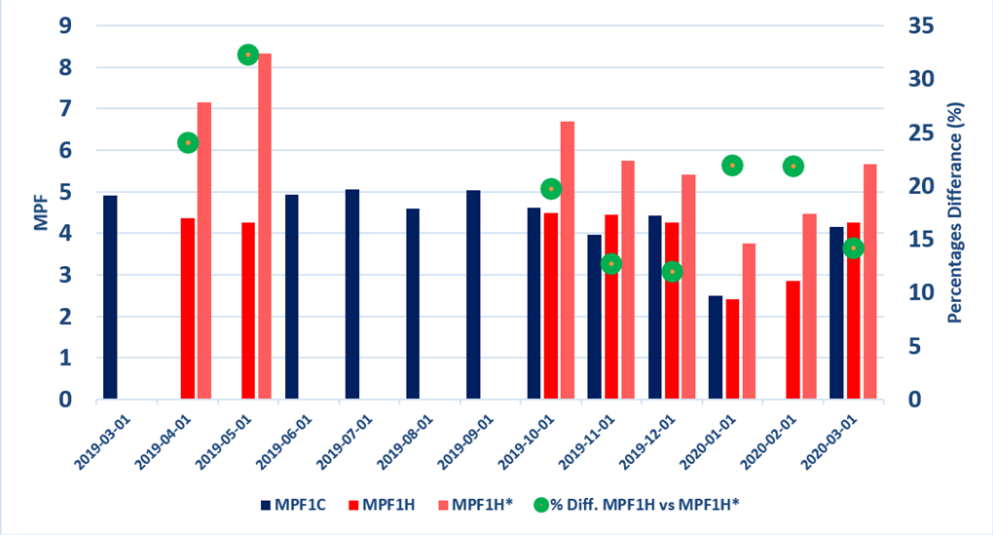

Figure 5: Monthly Performance Factor of Heat Pump Unit.

Using SPF_1 for the heat pump unit would give insight on how well the heat pump component is operating. But when the aim is to evaluate the actual energy performance of the system in place, SPF_{1H}^* can have a more realistic and fair evaluation of the actual system operation performance since part the heat source to the heat pump is simultaneously used to provide cooling for the building.

SPF_2 system boundary includes the groundwater pumps, the main circulation pump, heat pumps compressor, circulation pumps that are near the heat pump evaporator (before the cold buffer tank) that are used to deliver energy to the heat pump source side (see **Error! Reference source not found.**).

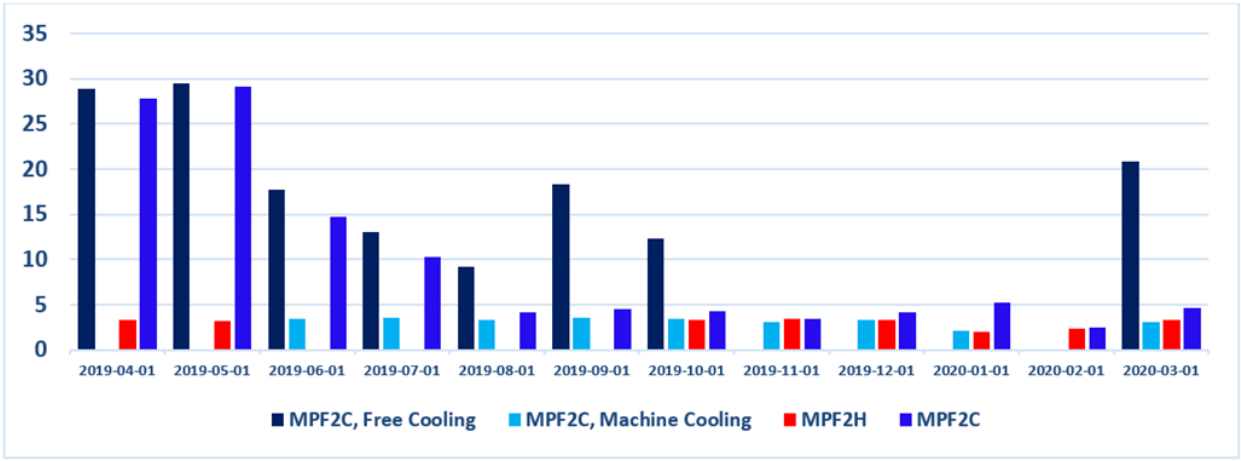

Figure 6: Monthly Performance Factor for the Second boundary level (MPF_2) which include the heat pump unit considering the building energy system operation modes.

In **Error! Reference source not found.**, $MPF_{2C,\ FreeCooling}$, $MPF_{2C,MachineCooling}$ refer to the performance factor when the system operating in free cooling only and machine cooling only respectively where MPF_{2C} refers to the performance factor of both free cooling and machine cooling. Similarly, MPF_{2H} refers to the performance factor when the system is operating in heating mode. The monthly average values of MPF_{1C} & MPF_{1H} are approximately 19 and 3 while the average value of the combination of both (MPF_{2C}) is around 9.5. These values are based on the assumption that all heat rejected from the condenser side of the heat pump is being rejected to the chiller on the roof and not used for heating the building. For heating mode, MPF_{2H} value is around 3. These values do not take into account the fact that the heat pump provides both heating and cooling at the same time given that to obtain such information, one would need to exceed the boundary of levels specified in **Error! Reference source not found.**. This suggests that those MPFs are likely to underestimate the actual MPF value when the system is operating heating and cooling simultaneously. For instance, when simultaneous heating and cooling is taken into account, MPF_{2H} monthly values would have an average increase of 20%.

Given that the heat pump is the main supplier of heat during the heating mode operation, the compressors had the majority share of the total electric energy consumed accounting for around 80%. On the other hand, the total electric energy consumption during the cooling operation was equally dominated by the groundwater pumps and circulation pumps taking around 35-50% and 50-65% respectively during free cooling mode. When machine cooling is used the compressor share of electrical energy consumption ranged 50-80% while the rest (20-50%) was equally shared between the ground water pumps and circulation pumps.

4.2 ATES Performance

The ground source loop (ATES) operation is evaluated in the first system boundary (SPF0). The operation of the ATES started since October 2016. Therefore, the ATES has completed three annual (heating and cooling) and a half storage cycle until end of March 2020 shown in **Error! Reference source not found.**. Annually on average, ATES energy injection (summertime) and extraction (wintertime) are 248 MWh and 158 MWh respectively.

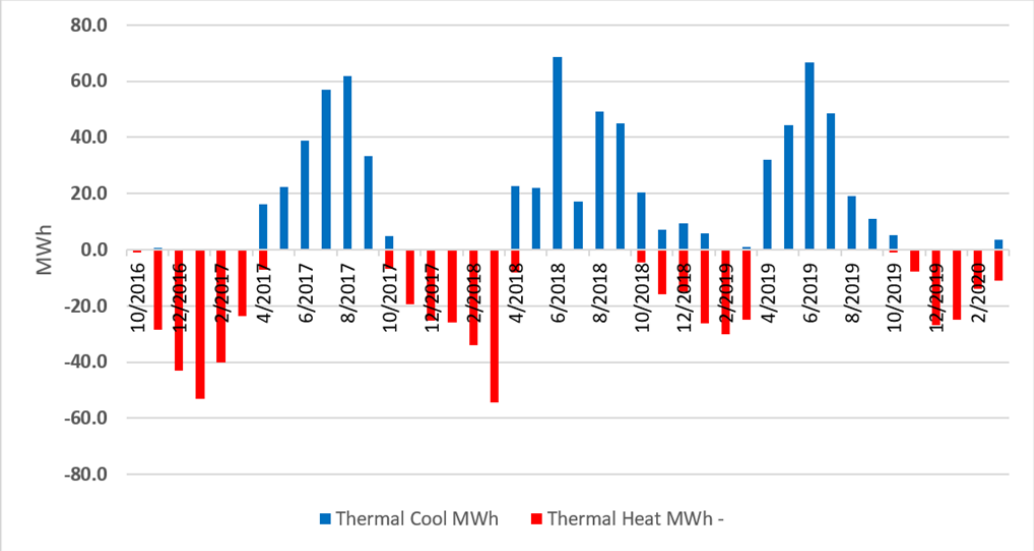

Figure 7: Monthly thermal energy exchange with the ATES during heating and cooling mode in MWh.

The evaluation of only $\boldsymbol{SPF_0}$ has been possible since 2016 given the data availability for the groundwater pumps ($\boldsymbol{W_{GWP}}$) and the main circulation pump ($\boldsymbol{W_{MCP}}$). Heating and cooling monthly performance factors ($\boldsymbol{MPF_0}$) values for the ATES are presented in **Error! Reference source not found.**. $\boldsymbol{MPF_0}$ values for cooling ranges between 73 and 11.

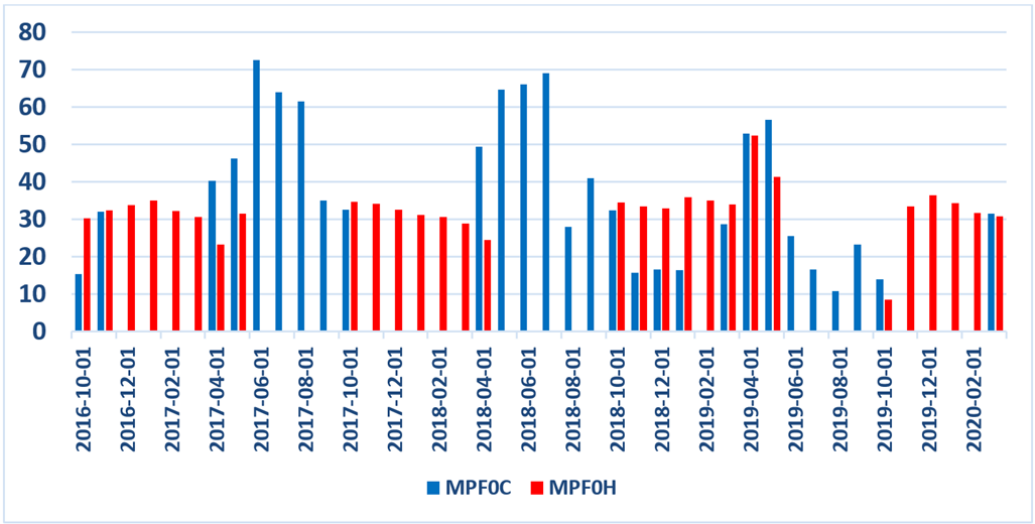

Figure 8: Monthly Seasonal Performance Factor for ATES (MPF0).

$\boldsymbol{MPF_{0C}}$ values have decreased over the years. Compared to the first years of operation, an average monthly decrease in $\boldsymbol{MPF_{0C}}$ values by 34% and 43% is measured in the last summer season. This indicates suboptimal utilization of the ATES or unsuitable choices for the

flow rates and temperature difference on both sides of the main heat exchanger connecting the ATES and the building heat and cooling system network. In contrast, $\boldsymbol{MPF_0}$ for heating values have been more consistent over the years averaging 33. This indicates a more suitable operation in terms of flowrates and temperatures differences (compared to summertime) during winter over the years. Given the high potential $\boldsymbol{MPF_0}$ values, more optimized ATES operation in connection to the system would have a significant impact on the overall performance. Therefore, optimizing the ATES operation should be prioritized to utilize its full potential when operating the heating and cooling system as a whole. The relative decrease in $\boldsymbol{MPF_{0C}}$ values can attributed mainly to the imbalanced yearly operation of the ATES and suboptimal choice of groundwater flow (often too high) and temperatures differences (often too low).

During summertime, total energy used from ATES has increased (235 to 272 MWh) during the first three summer seasons. In contrast, the use of heating energy during wintertime has decreased from 189 to 83 MWh near the end of the fourth heating season. A similar trend can be seen for the ground water volume used during heating operation which decreased from 37,000 to 13,000 m^3. In contrast, the ground water volume utilized during cooling has increased from 49,000 to 112,000 m^3 during the first 3 cooling seasons of operation. Most of the energy used during the fourth year was for heating since the data analyzed in this work is until March 2020 (**Error! Reference source not found.**)

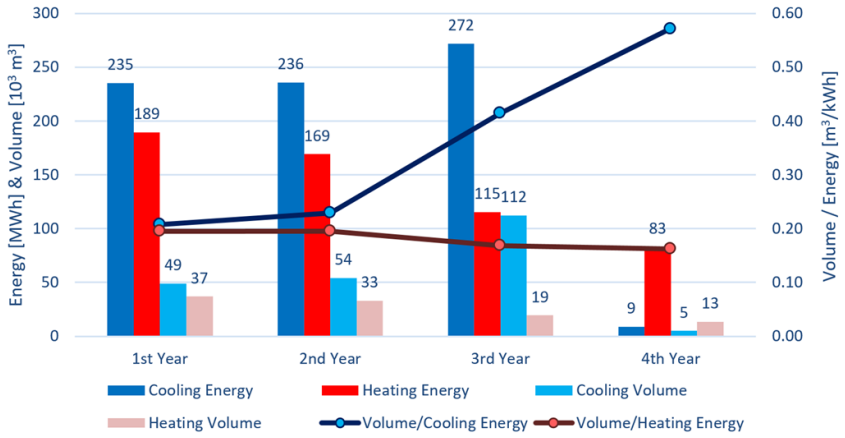

Figure 9: Total yearly energy [MWh] and water volume [10^3 m^3] used from the ATES (left axis) to heat and cool the building and the volume extracted per unit of energy [m^3/kWh] (right axis) during the period Oct 2016-March 2020. (Abuasbeh et al., 2021)

The ATES has experienced an imbalanced operation the years that resulted in a gradual temperature increase in the ATES as shown in table 2.

Table 2: Average extraction and injection temperatures, groundwater volume and temperature differences on the ATES during each heating and cooling season.

Season	1st heating	1st cooling	2nd heating	2nd cooling	3rd heating	3rd cooling	4th heating
T_{ext} [°C]	10.4	9.7	12.2	10.7	12.9	11.1	13.0
T_{inj} [°C]	6.3	12.9	7.9	13.3	8.0	13.5	8.1
ΔT_{ATES} [K]	4.2	3.2	4.4	2.6	4.9	2.4	4.9
V [m^3]	37,000	49,000	33,000	54,000	19,000	112,000	13,000

The heat exchanger efficiency ($\boldsymbol{\eta_{HEX}}$) describes how much of the maximum possible temperature difference across the heat exchanger has been utilized. **Error! Reference source not found.** shows that the average yearly values for the heat exchanger efficiencies from building side ($\boldsymbol{\eta_{HEX_{build}}}$) range between 0.94 to 0.99 during cooling and 0.86 to 0.82 during heating operation. For the ATES side, $\boldsymbol{\eta_{HEX_{ATES}}}$ values range between 0.60 to 0.47 during cooling and 0.76 to 0.79 during heating. It also shows that the efficiencies from the building side are consistently higher than ATES. Ideally, the values from both the ATES and the building side should be as high and as similar in their values as possible for the same operation mode. The values during the heating operation are relatively similar with difference decreasing between them from the first to the fourth year of operation. This suggested that the operation of the heating system together with the ATES has maximized the temperature difference both on the building side ($\Delta \boldsymbol{T_{buildng}}$) and the ATES side ($\Delta \boldsymbol{T_{heating}}$).

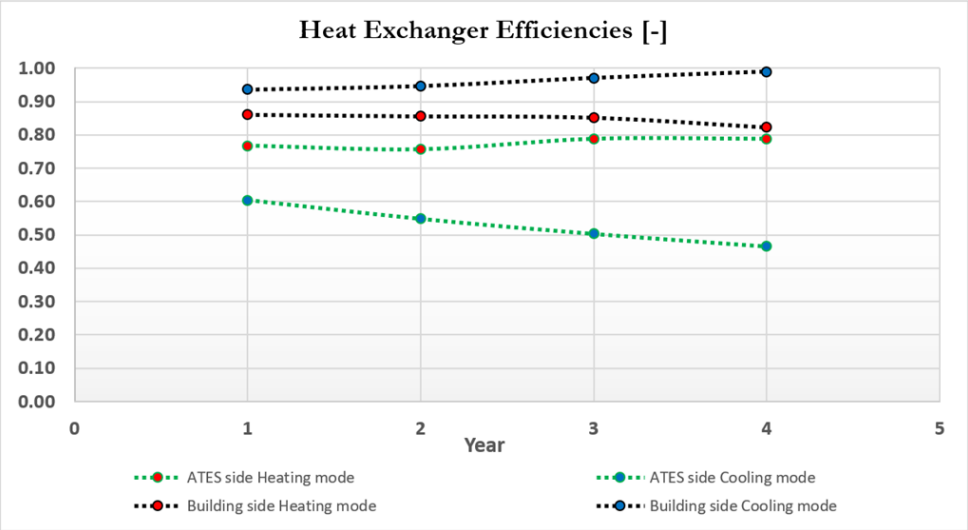

Figure 30: Heat exchanger efficiencies for both the building side ($\eta_{HEX_{build}}$) in the black line and the ATES side ($\eta_{HEX_{ATES}}$) during heating (red dots) and cooling (blue dots) modes.

In contrast, the values during the free cooling operation have significant and increasing difference between both sides of the heat exchanger. This suggested that the operation of the cooling system has been conducted so that it can maximize the temperature difference on the building side ($\Delta T_{buildng}$) to reach a suitable temperature for free cooling. This was on the expense of the temperature difference on the ATES side ($\Delta T_{heating}$) which was too low. Consequently, more ground water flowrate has been used to exchange the needed energy.

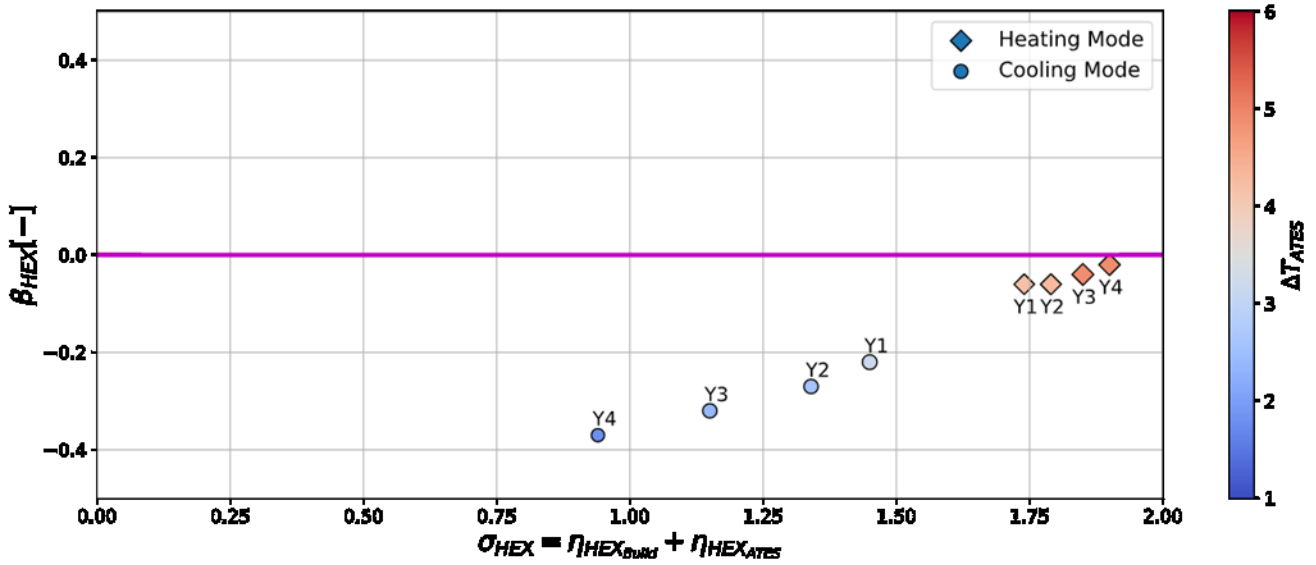

Figure 41: Heat exchanger efficiencies balance (β_{HEX}) vs the summation of the heat exchanger efficiencies (σ_{HEX}) for both the building side ($\eta_{HEX_{build}}$) and the ATES side ($\eta_{HEX_{ATES}}$) during heating (diamonds) and cooling (circles) modes.

The notation ***Y1***, ***Y2***, ***Y3*** and ***Y4*** refer to the years from 1st to the 4th year of operation. The color bar represent the temperature difference between the inlet and the outlet of the heat exchanger on the ATES side.

In addition to reaching a suitable forward temperature towards the building heating and cooling system, the choice of water flowrate on the building side should be optimized to also take into account maximizing the temperature difference on ATES side to minimize the ground water volume per unit of energy exchanged to minimize the potential of thermal breakthrough. **Error! Reference source not found.** shows that an optimum operation point would be when σ_{HEX} is approaching 2 (which is the maximum theoritical value) and β_{HEX} is approaching 0. When β_{HEX} value is approaching 0, this suggests that operation of the whole system equally considering the temperatrue difference on both the building and the ATES. When it comes to σ_{HEX}, a value approaching 2 suggests that the choice of the heat exchanger size and operational flowrate has been chosen to have the maximum possible temperature differences on both the building and the ATES side. **Error! Reference source not found.** contributes to understand if building heating and cooling system operational strategy has impacted the thermal recovery values from the ATES. For instance, we can see that the heating operation values in **Error! Reference**

source not found. are rather close to the optimum possible operation point being able to maximize the temperature difference on both the building and the ATES side. In such case, the main contributing factors for having heating thermal recovery efficiency for values below 1 are mostly related to the lack of heating demand or heat being lost to the surroundings and less related to system operation protocols. On the other hand, in the case of cooling operation, increasing imbalance in $\boldsymbol{\beta_{HEX}}$ in favor of the building side efficiency ($\boldsymbol{\eta_{HEX_{build}}}$) is observed. This means that the control system in the heating and cooling system has been mainly operating to achieve the lowest forward temperature possible towards the building. This is done without considering maximizing the temperature difference on the ATES side despite the fact that the efficiency of the heat exchanger on the ATES side ($\boldsymbol{\eta_{HEX_{ATES}}}$) did not exceed 60% even in the very first year of cooling operation. This was prior to any thermal breakthrough. $\boldsymbol{\eta_{HEX_{ATES}}}$ has further decreased even more down to 47% by the fourth year. In the following years, this became worse with the increase in the extraction temperatures from the cold side of the ATES caused by the thermal breakthrough. The color bar in **Error! Reference source not found.** shows the temperature difference between the inlet and the outlet of the heat exchanger on the ATES side. It shows that during the heating mode, the values of $\Delta \boldsymbol{T_{heating}}$ have been increasing from an average of 4 K up to around 5 K by the fourth heating season. This indicates a relatively efficient operation with additional room for improvement to further decrease the injection temperature in the cold side of the ATES especially after the first heating season. This is mainly to compensate for increased extraction temperatures from the warm side after the first heating season. During the cooling mode, the values of the temperature difference on the ATES side $\Delta \boldsymbol{T_{cooling}}$ have been relatively low from the very first cooling season and decreasing from around 3 K down to 1.8 K by the beginning of the fourth cooling season compared to the available 8K which is more desired value from the ATES prospective. In such case, thermal recovery efficiency for cooling has values below 1 meaning that the loss is not only caused by the subsurface hydrogeology, natural ground water movement or the amount of cooling demand, but rather the lack of suitable operational protocol for the system had a significant impact on the overall performance of the ATES.

5. CONCLUSION

Usually, we try evaluating the performance of subsystems by placing boundaries ($\boldsymbol{SPF_0}$, $\boldsymbol{SPF_1}$, $\boldsymbol{SPF_2}$, etc) to better explain the overall system performance. But in more complex systems (both in terms of component configuration and operation protocol) we are not able to accurately evaluate the performance of these subsystems solely based on the information within that boundary without the need for information from outside these boundaries.

By strictly following such component-based boundaries, especially on the lower levels such as SPF0 and SPF1, the performance values would give us a valuable insight into how well a particular component in the system is operating compared to the nominal or design value. In the other hand, this approach would lack the information about how this component is performing within the system which leads to inaccurate evaluation of the impact the system operation protocol has on the system levels performance. This study showed a potential underestimate of the actual system performance by up to 32%.

The main issue lays on the way to divide the electrical consumption of the various groundwater pumps, circulation pumps and compressors relative to the useful energy used. In particular, when the system is providing useful heating and cooling energy simultaneously. In such case, it is more reasonable to divide the total useful energy supplied (heating, cooling or both) by the corresponding electrical energy consumption. But when attempting to calculate the partial electrical consumption used of heating or cooling for a certain system boundary, it is sometime necessary to go beyond that boundary level in order to account for that.

The ATES, if operated in an optimal way, is by far the most efficient option to consider while heating and cooling (reaching MPF of more than 70). In this study case, from the ATES prospective, the heating and cooling system in the building has been operating in suboptimal way throughout the first 3 years of operation. This is highlighted by several indication such as, continuous imbalanced annual energy exchange with the ATES (much more cooling than heating), low temperature differences from the ATES side (4.7 K during heating and 2 K during cooling), and high (and increasing) extraction of groundwater volume per unit of energy.

This seems due to the heating and cooling system in the building controls the operation of the ATES in a way to achieve the maximum or minimum temperatures usable to be a heat source for the heat pump or cold source for free cooling. This led to extracting groundwater with temperature exceeding the undisturbed temperatures of the ATES. Although these temperatures are still suitable to be used for free cooling for the HVAC system, it will risk the ability to use the ATES for cooling in the future. Furthermore, due to that the heat pump capacity was too high, the district heating was used more than it was intended to, further reducing the chance to utilize the already available heat stored in the warm side of the ATES. This led to thermal breakthrough in the ATES from the warm to cold side.

The heat exchanger KPIs proposed can show how optimal the injection temperatures in the ATES were relative to the temperature difference available between the return line on the building side of the heat exchanger and the extraction line from the ATES. In our case, during the heating operation, the heat exchanger efficiencies were relatively closer the optimum point from the point of view of the building system and the ATES having $\boldsymbol{\eta_{HEX_{build}}}$ and $\boldsymbol{\eta_{HEX_{ATES}}}$ values around 84% and 79% on average. This indicates a rather more efficient operation protocol and the choice of flow rates on both sides of the heat exchanger. This resulted in average temperature difference on the ATES side of the heat exchanger $\Delta \boldsymbol{T_{heating}}$ was 4.7 K and about 5 K on the building side $\Delta \boldsymbol{T_{building}}$.

During the cooling operation, the heat exchanger efficiencies were significantly different and further away from the optimum point. From the point of view of the building system, $\boldsymbol{\eta_{HEX_{build}}}$ were relatively very high with values consistantly higher than 94%. In contrast, $\boldsymbol{\eta_{HEX_{ATES}}}$ values were relatively low and as low as 47%. This indicates the operation protocol and the choice of flow rates on both sides of the heat exchanger were aiming only to achieve the lowest forward temperature possible towards the building, which was evident by maintaining about 5 K on the building side $\Delta \boldsymbol{T_{build}}$, without considering the negative impact it has on the ATES represented in increased groundwater flowrate and decreased temperature difference on the ATES side $\Delta \boldsymbol{T_{cooling}}$ throughout the cooling operation over the years which ranged between 2.8 – 1.8 K. This is despite having 8 K difference in temperature between the building system's return line and the ATES cold

extraction line. The adjustment of increasing $\Delta T_{cooling}$ will help mitigate the thermal break through impact. This can be optimized by adjusting the flowrates on both sides of main heat exchanger, the use of large heat exchanger and including the a minimum limit of $\Delta T_{cooling}$ as well as maximum injection temperature into the cold side of the ATES. Higher temperature difference would result into smaller volume needed per unit of energy, which in turn would slow down the spread of the storage volume.

Furthermore, further study conducted on ATES-GSHP system coupling is of high significance in order to optimize the system operation as a whole and achieve long-term sustainable operation for the ATES.

ACKNOWLEDGEMENTS

Special thanks to the Swedish Energy Agency (Energimyndigheten,) for funding this research within Effsys Expand and TERMO research programs through Termiska Energilager, IEA HPT Annex 52 projects, and Sustainable Geothermal Energy for the Future: AI in ATES.

REFERENCES

Abuasbeh, M., & Acuna, J. (2018). *Ates system monitoring project, first measurement and performance evaluation: Case study in Sweden*. https://doi.org/10.22488/okstate.18.000002

Abuasbeh, M., Acuña, J., Lazzarotto, A., & Palm, B. (2021). Long term performance monitoring and KPIs' evaluation of Aquifer Thermal Energy Storage system in Esker formation: Case study in Stockholm. *Geothermics*, *96*, 102166. https://doi.org/10.1016/j.geothermics.2021.102166

Boman, D., & Hanson, G. (2004). *Salt grundvatten i Stockholms läns kust- och skärgårdsområden: Metodik för miljöövervakning och undersökningsresultat 2003*. Länsstyrelsen i Stockholms län. http://www.diva-portal.org/smash/record.jsf?pid=diva2:851965

de Wilde, P. (2014). The gap between predicted and measured energy performance of buildings: A framework for investigation. *Automation in Construction*, *41*, 40–49. https://doi.org/10.1016/j.autcon.2014.02.009

Energimyndighetens. (2020). *Energiläget 2020* (p. 99) [Statens energimyndighet]. Energimyndighetens. https://energimyndigheten.a-w2m.se/Home.mvc?ResourceId=168344

Gleeson, C. P., & Lowe, R. (2013). Meta-analysis of European heat pump field trial efficiencies. *Energy and Buildings*, *66*, 637–647. https://doi.org/10.1016/j.enbuild.2013.07.064

Imam, S., Coley, D. A., & Walker, I. (2017). The building performance gap: Are modellers literate? *Building Services Engineering Research and Technology*, *38*(3), 351–375. https://doi.org/10.1177/0143624416684641

Kurkinen, E.-L. (2014). *Skillnad mellan beräknad och verklig energianvändning—Energistyrning under byggprocessen-Slutrapport december 2014* (p. 39).

Liang, J., Qiu, Y., & Hu, M. (2019). Mind the energy performance gap: Evidence from green commercial buildings. *Resources, Conservation and Recycling*, *141*, 364–377. https://doi.org/10.1016/j.resconrec.2018.10.021

Menezes, A. C., Cripps, A., Bouchlaghem, D., & Buswell, R. (2012). Predicted vs. actual energy performance of non-domestic buildings: Using post-occupancy evaluation data to reduce the performance gap. *Applied Energy*, *97*, 355–364. https://doi.org/10.1016/j.apenergy.2011.11.075

Pérez-Lombard, L., Ortiz, J., & Pout, C. (2008). A review on buildings energy consumption information. *Energy and Buildings*, *40*(3), 394–398. https://doi.org/10.1016/j.enbuild.2007.03.007

Schmidt, T., & Müller-Steinhagen, H. (2004, June 20). The Central Solar Heating Plant with Aquifer Thermal Energy Store in Rostock—Results after four years of operation. *Eurosun*. Europe Solar Conference, Freiburg, Germany. http://www.solites.eu/download/literatur/04-05.pdf

Scofield, J. H. (2013). Efficacy of LEED-certification in reducing energy consumption and greenhouse gas emission for large New York City office buildings. *Energy and Buildings*, *67*, 517–524. https://doi.org/10.1016/j.enbuild.2013.08.032

Spitler, J. D., & Gehlin, S. (2019). Measured Performance of a Mixed-Use Commercial-Building Ground Source Heat Pump System in Sweden. *Energies*, *12*(10), 2020. https://doi.org/10.3390/en12102020

USEIA. (2020, June). *How much energy is consumed in U.S. buildings?* https://www.eia.gov/tools/faqs/faq.php

Vanhoudt, D., Desmedt, J., Van Bael, J., Robeyn, N., & Hoes, H. (2011). An aquifer thermal storage system in a Belgian hospital: Long-term experimental evaluation of energy and cost savings. *Energy and Buildings*, *43*(12), 3657–3665. https://doi.org/10.1016/j.enbuild.2011.09.040

WSP. (2014). *Miljökonsekvensbeskrivning: Akvifärlager Rosenborg 3, Solna stad. Ansökan om tillstånd för vattenverksamhet.* http://hydrologie.org/redbooks/a154/iahs_154_04_0068.pdf